2005 International Symposium on Nonlinear
Theory and its Applications (NOLTA2005)
Bruges, Belgium, October 18-21, 2005

Steady State Behavior of a Class of Periodically Perturbed Systems

Barry O'Donnell†, Paul F. Curran† and Orla Feely†

†Department of Electrical and Electronic Engineering,
University College Dublin, Belfield, Dublin 4, Ireland.
Email: barry.odonnell@ee.ucd.ie , paul.curran@ucd.ie , orla.feely@ucd.ie

Abstract—This paper examines the steady state behavior of a class of periodically perturbed mappings. This class displays a generalized periodicity and is characterized in the steady-state by an invariant set, or belt, of points of period-n. The rate of convergence to these belts and the thickness of the belt is seen to be influenced by the frequency of the perturbation. Furthermore, when the perturbation frequency equals π rad/s, generalized period-n behavior, where n is even, reduces to period-n behavior.

1. Introduction

This work examines behavioral aspects of a class of differentiable mappings. In [1], [2] and [3] the problem of perturbed period-doubling bifurcations has been investigated with particular emphasis on Josephson junctions. However, in all cases, many assumptions are made on the actual system. Furthermore, the authors report conflicting predictions that are valid only for extremely small values of the perturbation amplitude (many orders of magnitude smaller than the perturbation amplitudes considered here). This work investigates steady state behavior of a class of periodically perturbed mappings. A member of this class which formed the motivation for this work is the first-order Digital Phase-Locked Loop [4] described by the equation

$$\phi_e(n) = \phi_e(n-1) + 2\pi\nu + \alpha sin[\omega n + \theta_0] \\ -2\pi K_1(sin(\phi_e(n-1)) + \delta) \mod(2\pi) \quad (1)$$

where the term $\alpha sin[\omega n + \theta_0]$ is a modulating input and is the perturbation for this system. A bifurcation diagram of (1) is shown in Figure 1, where the steady-state phase error, ϕ_e, is found for varying values of K_1. It can be seen that the fixed point of the unperturbed system (α=0) undergoes a period doubling at the point K_1=0.333 as shown by the grey line. If the system (1) has a modulating input, ($\alpha \neq 0$), then the associated attractor of the perturbed system is characterized in the steady state by a 'belt' of points as shown by the black region of Figure 1. The belt is a contained in the ω-limit set. The unperturbed system is characterized by a fixed point (single grey line) in region 1 of Figure 1. The perturbed system is characterized by a single compact belt in the same region. We call this a generalized period-1 solution. Similarly, for the period-2 cycle of the unperturbed system, (region 2), there is a compact and disconnected belt made up of two connected pieces for the perturbed system. The points on this belt cycle in a certain way, i.e. starting with an initial point on one of the pieces, this point jumps from one piece to the next each iteration. Furthermore, this belt is such that if the size of the perturbation becomes arbitrarily small then the period-2 solution is recovered. We call this a generalized period-2 solution for the perturbed system and the associated attractor is denoted a belt of period-2. Furthermore, for the period-4 cycle of the unperturbed system, (region 3), there is a generalized period-4 solution for the perturbed system. In other words, the belt of the perturbed system has periodicity of the underlying unperturbed system.

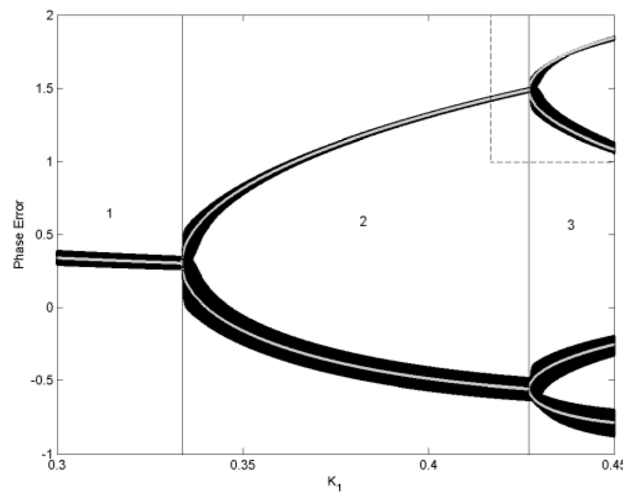

Figure 1: Bifurcation Diagram of the system (1) with ν=0.1, ω=0.005, δ=0, α=0 (grey) and α=0.08 (black)

As shown in [5], equation (1) is a member of a much larger class of mappings having the form,

$$x(n) = F_q(x(n-1)) = F(x(n-1)) + q(n-1), \quad q(n-1) \in [-\alpha, \alpha] \quad (2)$$

where $F(x)$ is differentiable on some interval I. We denote this class $\mathcal{F}$ where,

$$\mathcal{F} = \{F_q | q(n-1) \in [-\alpha, \alpha]\} \quad (3)$$

This is a robust class as q can model any perturbation such as jitter, noise, modulating input etc. However, this paper will consider some interesting steady state behavior of the class (3) when restrictions are placed on the perturbation sequence $q(n-1)$ of (2).

The rate at which an interval of points converges to the attracting belt will be seen to depend on the perturbation sequence. Moreover, for appropriate choice of perturbation frequency one can achieve near instant convergence to the belt of given period. Furthermore, if there exist constraints on the perturbation sequence then the thickness of a belt of given period depends on the perturbation frequency. A special dependency reveals how generalized period-n behavior, where n is even, can vanish and be replaced by period-n behavior. This result is used to clearly illustrate the strict ordering result of [5], i.e. that belts of period-n of the perturbed system (2) never lose stability after the period-n cycles of the associated unperturbed system.

2. Rate of Convergence to Belt

As previously mentioned, the class (3) is a robust class as the perturbation term, q, can model any perturbation such as jitter, noise, modulating input etc. For the case of the modulating input (1), the perturbation sequence is deterministic (unlike the case of noise and jitter) and is set by the modulating frequency, ω. In Figure 2 the line 'Phase error - U^*=0' corresponds to the upper limit of the attracting belt. This Figure shows that under the twice iterated map of (1) the convergence of the upper bound of a larger interval to the belt differs for various constraints on the perturbation sequence. Only the first iteration is shown in this analysis. The '•' symbol illustrates the case when the perturbation sequence switches sign every iteration with the starting value of the sequence positive. It shows that for one application of the twice iterated map of (1) the upper bound of the interval converges to the upper bound of the belt. The '×' symbol represents the case when the perturbation sequence is approximately constant and positive. For this case it can be seen that after a single iteration the image of the upper bound of the interval is located inside the belt. In fact, it is located at a point 0.0185 below the upper bound of the belt. This indicates instant convergence to the belt. Similarly, the two remaining cases also experience instant convergence. These cases are when the perturbation sequence is approximately constant and negative ($*$) and when the perturbation sequence switches sign every iteration with the starting value of the sequence negative (+). The image of the upper bound of the interval lies at a distance below the upper bound of the belt equal to 0.0244 for the (*) case and 0.0481 for the (+) case. These results will be shown to be in good agreement with theoretical analysis. For simplicity, we will look at the twice iterated map of the following generalized system,

$$\phi_{n+1} = G(\phi_n) = F(\phi_n) + f(\omega n + \theta_0) \quad \text{and} \quad \phi^* = F(\phi^*) \quad (4)$$

where $\theta_n = \omega n + \theta_0$, $|f(\theta)| \leq \alpha$ for all θ and f is 2π periodic. This is a special case of (2) where the perturbation sequence has frequency ω and is N periodic if $\omega = 2\pi m/N$ for integer m. It will be shown that for suitable choice of ω the convergence of a larger interval to the belt, where the

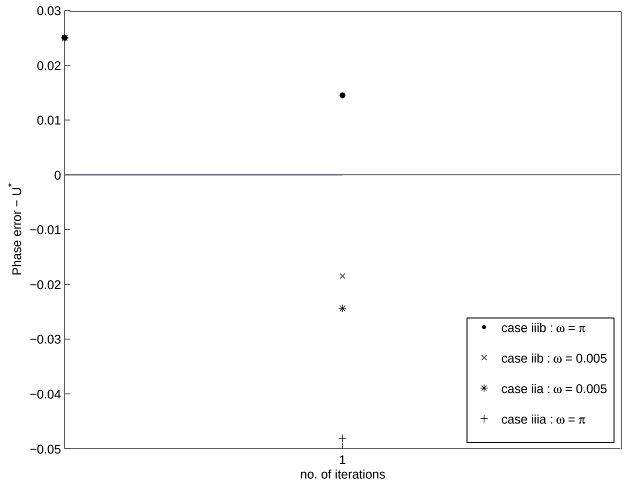

Figure 2: Convergence of upper bound to the belt under twice iterated map of system (1). ζ=0.025, ν=0.1, K_1 =0.3, δ=0, α=0.02.

larger interval contains the belt, can be maximized. First, we reintroduce a definition from [5].

Definition 1- A Fixed Interval I^* of class (3) is a compact interval which is invariant under the class (3), i.e. I^* is the minimal set such that F_q maps I^* into I^* for all $q \in [-\alpha, \alpha]$.

Let the fixed interval $I^* = [L^*, U^*]$ and let $I = [L^* - \zeta,\ U^* + \zeta]$ be a larger interval where $\zeta > 0$. For convenience, the convergence of the points $L^* - \zeta,\ U^* + \zeta$ to the points $L^*,\ U^*$ under the twice iterated map is examined.

Monotone decreasing case: This is the case when F is monotone decreasing on I. The first-order DPLL of (1) is a special case of this. From definition 1, I^* is invariant under F_q for all $q \in [-\alpha,\ \alpha]$. Therefore the image of the points L^* and U^* under the mapping F_q are,

$$\begin{aligned} U^* &= F(L^*) + \alpha \\ L^* &= F(U^*) - \alpha \end{aligned} \quad (5)$$

and $|I^*| \geq 2\alpha$, Also, $-1 < -\mu \leq DF(\phi) < 0$, where DF denotes the Jacobian of F and $\phi \in I^*$.
The convergence of the points $L^* - \zeta,\ U^* + \zeta$ under the twice iterated map of (4) (see appendix) is examined for various conditions on the perturbation sequence. These points are mapped to some point in a bounding interval as indicated in the following cases.
(i) $f(\theta_n)$ and $f(\theta_{n+1})$ can attain any value in $[-\alpha,\ \alpha]$, then,

$$\begin{aligned} G(G(U^* + \zeta)) &\in [U^* - 2\alpha(1 + \mu),\ U^* + \mu^2\zeta] \\ G(G(L^* - \zeta)) &\in [L^* - \mu^2\zeta,\ L^* + 2\alpha(1 + \mu)] \end{aligned} \quad (6)$$

This says that if there are no restrictions on the perturbation sequence then the point $U^* + \zeta$ is mapped to some point in the interval $[U^* - 2\alpha(1 + \mu),\ U^* + \mu^2\zeta]$. Similarly, the point $L^* - \zeta$ is mapped to some point in the interval $[L^* - \mu^2\zeta,\ L^* + 2\alpha(1 + \mu)]$.

The following cases highlight some interesting results when restrictions are placed on the perturbation sequence.
(iia) $f(\theta_n) \simeq f(\theta_{n+1})$ and negative, then,

$$\begin{aligned} G(G(U^* + \zeta)) &\in [U^* - 2\alpha,\ U^* - \alpha] \\ G(G(L^* - \zeta)) &\in [L^*,\ L^* + \alpha(1 + \mu)] \end{aligned} \tag{7}$$

The interval $[L^* - \zeta,\ U^* + \zeta]$ is sent instantly into the fixed interval under the twice iterated map. The convergence of $U^* + \zeta$ is confirmed by the '$*$' symbol in figure 2.
(iib) $f(\theta_n) \simeq f(\theta_{n+1})$ and positive, then,

$$\begin{aligned} G(G(U^* + \zeta)) &\in [U^* - \alpha,\ U^*] \\ G(G(L^* - \zeta)) &\in [L^* + \alpha,\ L^* + 2\alpha] \end{aligned} \tag{8}$$

The interval $[L^* - \zeta,\ U^* + \zeta]$ is sent instantly into the fixed interval under the twice iterated map. The convergence of $U^* + \zeta$ is confirmed by the '$\times$' symbol in figure 2.
(iii) $f(\theta_n)$ and $f(\theta_{n+1})$ are opposites of each other, then,
(iiia) $f(\theta_n) = \alpha = -f(\theta_{n+1})$,

$$\begin{aligned} G(G(U^* + \zeta)) &\in [U^* - 2\alpha(1 + \mu),\ U^* - 2\alpha] \\ G(G(L^* - \zeta)) &\in [L^* - \mu^2\zeta,\ L^*] \end{aligned} \tag{9}$$

The point $U^* + \zeta$ is mapped instantly into the fixed interval under the twice iterated map, whereas the point $L^* - \zeta$ may not as indicated by the $\mu^2\zeta$ term. The convergence of the term $U^* + \zeta$ into the fixed interval is confirmed by the '+' symbol in figure 2.
(iiib) $f(\theta_n) = -\alpha = -f(\theta_{n+1})$,

$$\begin{aligned} G(G(U^* + \zeta)) &\in [U^*,\ U^* + \mu^2\zeta] \\ G(G(L^* - \zeta)) &\in [L^* + 2\alpha,\ L^* + 2\alpha(1 + \mu)] \end{aligned} \tag{10}$$

The point $L^* - \zeta$ is mapped instantly into the fixed interval under the twice iterated map, whereas the point $U^* + \zeta$ may not as indicated by the $\mu^2\zeta$ term. The μ^2 dependence is highlighted in figure 2 by the '•' symbol. The numerical results agree qualitatively and quantitatively with the theory. The analysis shows that cases (iia) and (iib) provide instant convergence of the upper and lower bound of the larger interval to the fixed interval under the twice iterated map of the (4). This is confirmed by the numerical results seen in figure 2.
The monotone increasing case follows the same procedure however, due to space restrictions, is not included in this paper.

3. Effect of ω on Size of Belt of Period-2

In this section, it will be shown that if the perturbation sequence changes by regular amounts every iteration then the size of the belt of given period can be seen to vary in thickness. As explained in section 2, the modulating frequency, ω, controls the perturbation sequence for the special case (1). Figure 3 shows a steady state phase error diagram of phase error for varying values of modulating frequency, ω. This is for K_1=0.42 which indicates that the system (1) is operating in the period-2 attractor region (region 2 of Figure 1). If successive perturbation values are allowed to attain any value in the range $[-\alpha,\ \alpha]$ then the steady state phase error will lie in the range

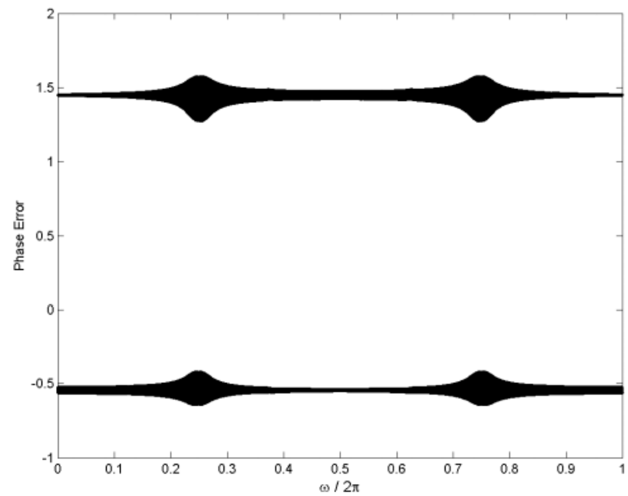

Figure 3: Steady State Phase Error of the system (1) with ν=0.1, K_1=0.42, δ=0, and α=0.02

$$\begin{aligned} \phi_{n+1} \in [&(F \circ F)(\phi_{n-1}) - \alpha(DF(V'_{n-1}) + 1), \\ &(F \circ F)(\phi_{n-1}) + \alpha(DF(V'_{n-1}) + 1)] \end{aligned} \tag{11}$$

where $V'_{n-1} \in [F(\phi_{n-1}),\ F(\phi_{n-1}) + u_{n-1}]$, $-\alpha \le u_{n-1} \le \alpha$. If, however, the perturbation frequency is ω rad/s then the steady state phase error will lie in the range,

$$\begin{aligned} \phi_{n+1} \in [&(F \circ F)(\phi_{n-1}) - \alpha(DF(V'_{n-1}) - 1), \\ &(F \circ F)(\phi_{n-1}) + \alpha(DF(V'_{n-1}) - 1)] \end{aligned} \tag{12}$$

which is a smaller interval than that of (11). This indicates that by appropriate choice of perturbation frequency the size of the belt can vary in thickness. Figure 3 shows the effect that ω has on the size of the belt. It can be seen for ω small that the width of the belt is minimized. However, as ω increases the width of the belt increases and reaches a maximum at $\omega = \pi/2$. As ω is increased further there is a contraction in the thickness of the belt. The thickness of the belt experiences a further expansion as ω approaches $3\pi/2$ and contracts again for ω approaching 2π. This expansion and contraction repeats every 2π rads.

4. Special Case: ω equals π rad/s

Consider system (1). With $\omega = \pi$ rad/s and the system operating in the generalized period-1 region (region 1 of Figure 1) then the steady state oscillates between two points. Where before there was an invariant belt there are now two points. In the generalized period-2 region of figure 1, (region 2), it can be shown that if $\omega = \pi$ rad/s then successive terms, $f(\theta_n)$ and $f(\theta_{n-1})$, cancel and the steady state ϕ_e oscillates between two points. Where before there was a compact belt made up of two disconnected pieces there are now two points. This is an interesting result and indicates that when ω equals π rad/s for system (4), generalized period-*n* behavior, where *n* is even, vanishes and is replaced by period-*n* behavior. In general, if $\omega = \pi$ rad/s for system (4), belts of period-*n*, where *n* is odd, reduce to points of period-2*n*. Furthermore, belts of period-*n*, where *n* is even, reduce to points of period-*n*. Figure 4 shows part of the bifurcation diagram of the system (1) where the phase error is calculated for varying values of K_1. In particular it shows where the upper bound of the period-2 attractors loses stability in a pitchfork bifurcation. This region is indicated by the dashed box section of Figure 1. When $\omega = \pi$ rad/s the belt of period-2 reduces to points of period-2 as indicated by the black line in Figure 4. It is clear that the point at which the perturbed system loses stability is to the left of the unperturbed system (grey line). This observation supports the main result of [5] which proved that belts of period-*n* of the perturbed system (2) never lose stability after the period-*n* cycles of the associated unperturbed system.

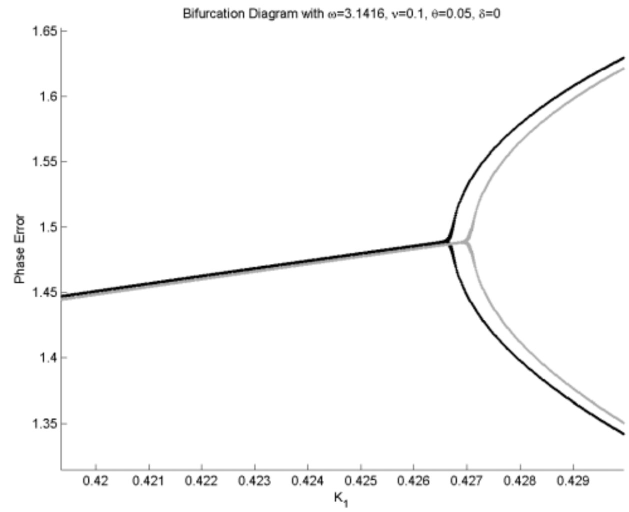

Figure 4: Bifurcation Diagram of the system (1) with ν=0.1, ω=π, δ=0, α=0 (grey) and α=0.04 (black)

Conclusions

This paper has looked at some interesting steady state behavior of the class of perturbed mappings (3). In particular it was shown that certain behavior is dependent on the perturbation sequence, q_{n-1} of (2). Firstly, the rate at which an interval of points converges to the attracting belt can be maximised for a certain choice of perturbation frequency. Secondly, the thickness of a belt of given period is dependent on the perturbation frequency. A special case of the perturbed system showed how generalized period-*n* behavior, where *n* is even, can be replaced by period-*n* behavior. This result served to illustrate the findings of [5] that belts of period-*n* of the perturbed system (2) never lose stability after the period-*n* cycles of the associated unperturbed system.

Appendix

The twice iterated map of (4) in the monotone decreasing case is given by :

$$(U^* + \delta) \rightarrow$$
$$U^* - \alpha + DF(\hat{\phi}_u)(\alpha + DF(\phi_u)\delta + f(\theta_n)) + f(\theta_{n+1}) \quad (13)$$
$$(L^* - \delta) \rightarrow$$
$$L^* + \alpha - DF(\hat{\phi}_l)(\alpha + DF(\phi_l)\delta - f(\theta_n)) + f(\theta_{n+1}) \quad (14)$$

where,

$$U^* \leq \phi_u \leq U^* + \delta$$
$$L^* \leq \hat{\phi}_u \leq L^* + \alpha + DF(\phi_u)\delta + f(\theta_n)$$
$$L^* - \delta \leq \phi_l \leq L^*$$
$$U^* - \alpha - DF(\phi_l)\delta + f(\theta_n) \leq \hat{\phi}_l \leq U^* \quad (15)$$

References

[1] H. Svensmark, M.R. Samuelsen, "Perturbed period-doubling bifurcation. I. Theory", *Phys Rev.* B41, 4180 (1990).

[2] G.F. Eriksen, J.B Hansen, "Perturbed period-doubling bifurcation. II. Experiments on Josephson junctions", *Phys Rev.* B41, 4189 (1990).

[3] P. Bryant, K. Wiesenfeld, "Suppression of period-doubling and nonlinear parametric effects in periodically perturbed systems", *Phys Rev.* A33, 2525 (1986).

[4] A. Vasylenko, O. Feely, "Dynamics of phase-locked loop with FM input and low modulating frequency", *International Journal of Bifurcation and Chaos*, Vol. 12, No. 7 pp. 1633-1642, 2002.

[5] B. O'Donnell, P. Curran, O. Feely, "On the Bifurcation Properties of a Class of Differentiable Mappings", to be published in the *Proceedings of the 17th European Conference on Circuit Theory and Design (ECCTD),* 2005.

[6] R.C. Hilborn, "Chaos and Nonlinear Dynamics, An introduction for Scientists and Engineers", *Oxford University Press*, 1994.

[7] F.M. Gardner, "Frequency granularity in digital phase-locked loops", IEEE Trans. Commun., vol. 44, pp. 749-758, June 1996.